A Mechanistic Model for Sequential and Entangled Spin Correlations

The LGAM Proximal Correlation Model

Michael Hodges
Independent Researcher
Preprint Revised — 9-September 2026

Abstract

This paper extends the Liquid Gravity Atomic (LGA) framework (Hodges, 2026), in which electron spin emerges from structured nuclear dynamics rather than existing as an intrinsic electron property, into a fully specified, computationally tested mechanistic model. We present a step-by-step model, developed through iterative computational testing, that reproduces the quantum mechanical prediction for sequential spin measurement (the $\cos^2(\theta/2)$ transition probability) and, in an extension to the entangled two-particle case, the entangled-pair correlation underlying the CHSH form of Bell's inequality. In the sequential model, each measurement stage draws only on information available to a single, previously-measured particle, and is shown to satisfy same-setting invariance, rotational (reference-angle) consistency, and the three-stage measurement-disturbance effect predicted by standard quantum mechanics. The entangled-pair extension reproduces the correlation curve to within 2 percentage points across the full 0-180 degree range and yields a CHSH value of $S \approx 2.82$, closely approaching the theoretical quantum maximum of $2\sqrt{2} \approx 2.828$ — a value that exceeds the classical bound of 2 available to any model in which each particle's outcome depends only on its own local setting. We show, through direct numerical demonstration, that this result requires the shared origin-state of the two particles to depend on the eventual measurement setting of only one of the two detectors — a specific, minimal, and previously undescribed shared-value dependency that we term a Proximal Correlation Model. This shared value is generated from a trigger fixed at the particles' common origin and independent of either particle's own spin label, a requirement confirmed directly by explicit marginal-independence (no-signaling) testing across the full range of measurement settings. We distinguish this model from superdeterminism, Bohmian mechanics, and retrocausal accounts, and discuss its consistency with, and limitations relative to, the causal structure required by loophole-free Bell test experiments. We also describe the collaborative human-AI methodology used to develop this model, which we consider a relevant and reportable part of the research process.

1. Background: The Liquid Gravity Atomic Framework

This paper builds directly on the Liquid Gravity Atomic (LGA) framework, previously presented in full in Hodges (2026), which proposes that electron spin, wavefunction collapse, and entanglement can be explained as emergent consequences of structured nuclear dynamics rather than as intrinsic, irreducible quantum properties. We summarise the relevant elements of that framework here, both to make the present paper self-contained and because the mechanistic model developed in Sections 3 onward is, in effect, a direct computational implementation of the physical picture described below.

1.1 The Nuclear Origin of Electron Spin

In the LGA framework, all particles, fields, and forces are proposed to emerge from a single, ubiquitous medium possessing both fluid and elastic properties, with interactions carried by positive and negative pressure gradients within it. Charges arise as localised stretches or compressions of this medium; nucleons are modelled as high-energy pulses confined within a condensed superfluid region, adopting figure-eight (∞) standing-wave trajectories that produce alternating positive and negative eddies and vortex-tube structures.

Electron spin, in this picture, is not an intrinsic property of the electron but a driven, inherited behaviour, transmitted outward from the nucleus. Nucleons form linked multichain arrangements — a more structured configuration than the loosely bound collection of nucleons assumed by the conventional Liquid Drop Model. Both protons and neutrons undergo internal figure-8 standing-wave motion; the proton initiates a circulating positive field, and neutrons — while electrically neutral — receive and relay this positive field along proton-neutron chains. The terminal neutron in each chain couples the resulting oscillating field into the orbital region, and the electron, tethered to that orbital, inherits the field's characteristic two-turn, 720° rotational signature as its observed spin behaviour.

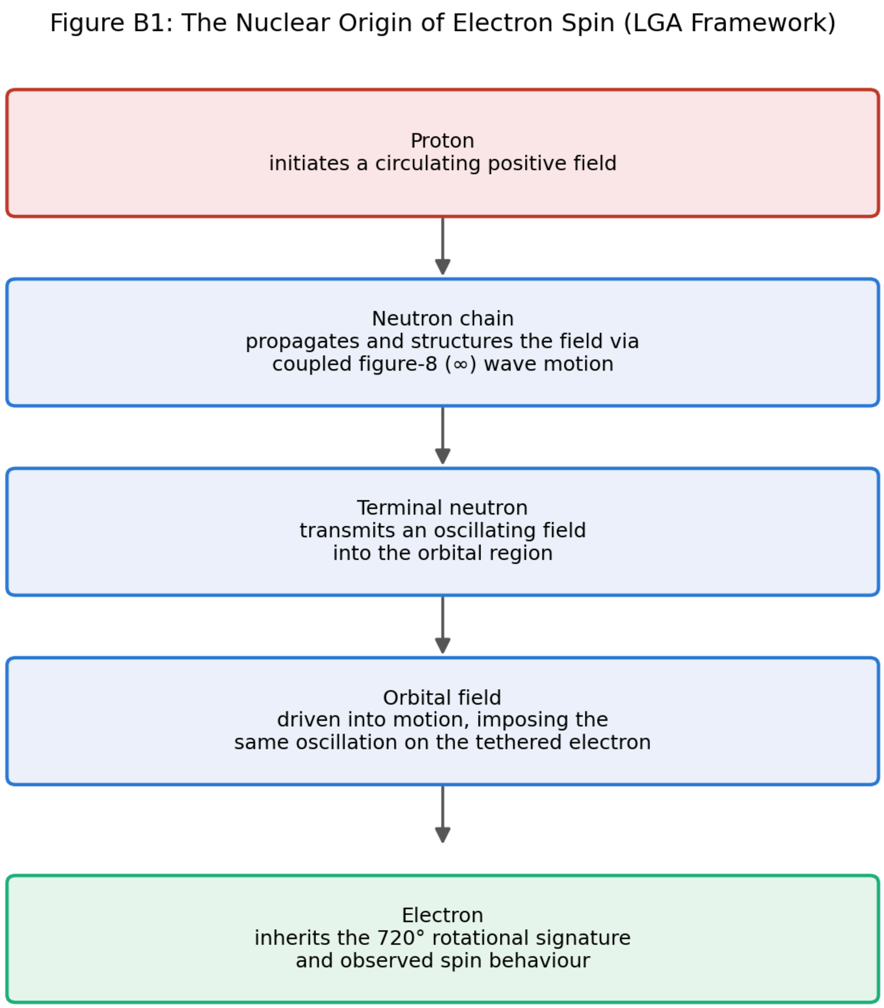

Figure B1. The proposed nuclear origin chain for electron spin, as described in Hodges (2026): a proton-initiated field is structured and relayed along a neutron chain, transmitted into the orbital region by the terminal neutron, and inherited by the tethered electron as its 720° rotational signature.

1.2 Superposition as Balanced Trajectory, Collapse as Trajectory Lock

The LGA framework further proposes specific physical accounts of superposition and wavefunction collapse, both grounded in the same figure-8 trajectory. In the absence of an external field, the neutron pulse propagates along a closed, balanced double-loop figure-eight trajectory, completing a 720° dual-wave cycle and passing through two negative field zones and one positive zone twice per cycle. The valence electron, confined within the resulting alternating field, oscillates correspondingly between the two hemispheres of the orbital; in this balanced state, no fixed spin orientation exists. What standard quantum mechanics describes as superposition is, in this framework, this alternating positional state — the spin orientation associated with each hemisphere flips every time the underlying trajectory crosses over.

Collapse, correspondingly, is proposed to result from a specific physical sequence: an external magnetic field competes with the electron's local, nuclear-driven field, geometrically consolidating (collimating) the electron's spatial distribution; this consolidation increases the effective centrifugal influence on the neutron pulse, driving a dynamical transition from the balanced double-loop trajectory into a locked single-loop rotation. Because the resulting geometric configuration is centrifugally stabilised, this locked state persists even after the external field is removed — yielding a well-defined, persistent spin orientation without requiring an observer-dependent collapse postulate.

Spin-state reversal is proposed to follow a torque relationship tied to the pulse's position on its original figure-eight path: torque is minimal at the apex of the trajectory's negative zones and maximal at the crossover point, with reversal occurring when the externally applied magnetic torque exceeds the torque already present in the pulse's own motion.

1.3 Deriving the Flip Threshold from the Torque Relationship

Hodges (2026) proposes a torque relationship governing spin-state reversal (Section 9 of that work), in which the magnetic torque acting on the nucleon pulse follows $\tau_{magnetic}(\theta) = \tau_{max} \cdot \sin^2(\theta/2)$, where θ is the angle between the magnet and the pulse's position, with reversal occurring when this magnetic torque exceeds a competing, pulse-generated torque. We show here that this relationship, properly framed, derives — rather than merely motivates — the discrete flip-threshold rule used throughout the present computational model.

Treating the pulse-generated torque as the mirror complement of the magnetic torque, evaluated over the same relative angle — $\tau_{pulse}(\theta) = \tau_{max} \cdot \cos^2(\theta/2)$ — the reversal condition $\tau_{magnetic} > \tau_{pulse}$ becomes $\sin^2(\theta/2) > \cos^2(\theta/2)$. Applying the identity $\sin^2(x) - \cos^2(x) = -\cos(2x)$ with $x = \theta/2$, this simplifies to $\cos(\theta) < 0$, which holds if and only if $\theta > 90°$. The competing-torque relationship therefore derives, exactly, the $|rot| > 90°$ flip-threshold rule used throughout Section 4, rather than merely being consistent with it.

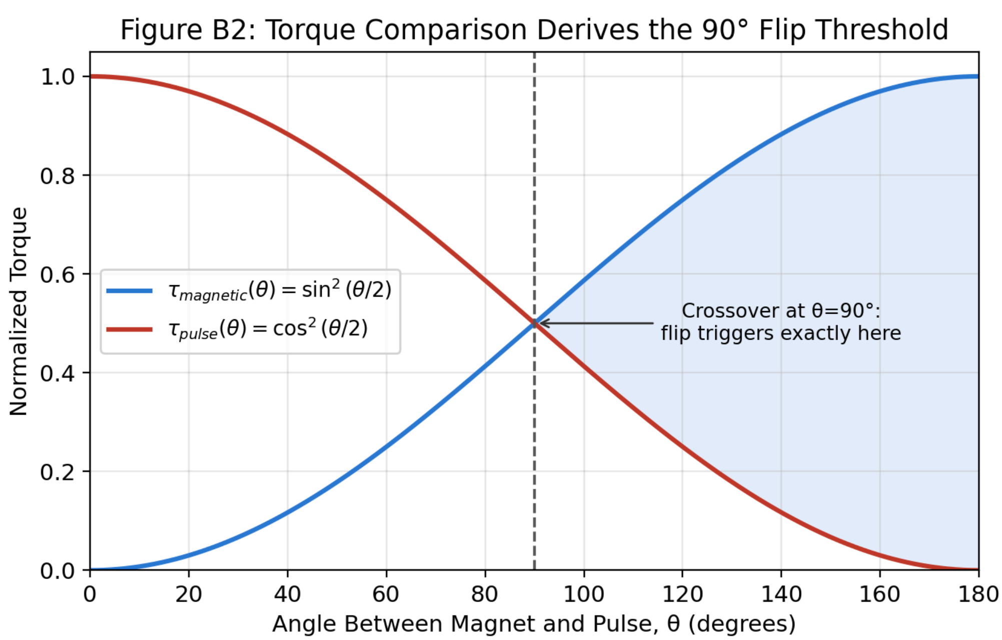

Figure B2. The magnetic torque (blue, $\sin^2(\theta/2)$) and the mirrored pulse-generated torque (red, $\cos^2(\theta/2)$) cross exactly at $\theta=90°$, the point at which the competing-torque condition changes sign — deriving the discrete flip threshold used throughout the present model directly from the torque relationship of Hodges (2026).

We verified this derivation numerically as well as algebraically: a two-stage sequential simulation implementing the explicit torque comparison (rather than the $|rot| > 90°$ threshold directly) reproduces the established results exactly, including 100.0% same-setting invariance at every angle tested and a curve matching the $\cos^2(\theta/2)$ target to the same precision reported in Section 5.1.

1.4 Relation to the Present Work

The mechanistic model developed in this paper (Section 4 onward) formalises this physical picture computationally: the Particle_Angle, Phase, and flip-threshold variables introduced below are a direct, testable implementation of the figure-eight trajectory, crossover-triggered reorientation, and 720° signature described above, and, as shown in Section 1.3, the flip threshold itself is a direct algebraic consequence of the competing-torque relationship proposed in Hodges (2026), rather than an independently motivated mathematical construction. Where the original framework described the mechanism qualitatively and proposed it as a physical account of spin, collapse, and entanglement, the present work subjects a precise, step-by-step version of that account to direct numerical verification against the specific quantitative predictions of quantum mechanics — the $\cos^2(\theta/2)$ transition probability and the CHSH inequality — reporting where it succeeds, where it required correction, and where open questions remain.

2. Introduction

Bell's theorem (Bell, 1964) establishes that no physical model in which measurement outcomes depend only on locally available information — the setting of the local measuring device and a hidden variable shared at the particles' common origin, but never on the distant, independently-chosen setting of the other measurement — can reproduce the full quantum mechanical correlation between entangled particles. This is quantified by the CHSH inequality (Clauser, Horne, Shimony, & Holt, 1969): any such local model is bounded by $|S| \leq 2$, while quantum mechanics predicts, and experiment confirms, a maximum value of $S = 2\sqrt{2} \approx 2.828$. This bound has been confirmed with progressively closed experimental loopholes, from the original photon-polarization experiments of Aspect, Grangier, and Roger (1982) through the loophole-free electron-spin test of Hensen et al. (2015), which used entangled electron spins in diamond nitrogen-vacancy centres separated by 1.3 kilometres.

As discussed in Section 1, Bell's theorem specifically excludes models in which each hidden variable determines a single, predetermined outcome for a given measurement setting. It does not, by itself, exclude models in which a locally-defined hidden variable, combined with a local measurement-angle parameter, produces genuinely probabilistic — rather than predetermined — outcomes. The present work investigates whether such a multi-parameter mechanism, built from information available at the particles' point of origin, can be constructed explicitly, in step-by-step computational form, and tested directly against the quantitative predictions that Bell-type experiments are designed to distinguish.

We report two results. First, a model of sequential spin measurement (one particle, measured twice, at two different magnet settings) that reproduces the quantum mechanical transition probability and several associated experimental facts, including the classical three-stage disturbance effect (the well-known result that an intervening measurement along an incompatible axis erases prior information about the measured particle's state). Second, an extension of the same mechanism to the entangled two-particle case, which we use to identify precisely where, and in what minimal form, a shared dependency between the two particles is required for the model to succeed.

A central methodological commitment of this work, maintained throughout its development, is that any formula reproducing a quantum mechanical prediction must be independently derived from geometric or threshold-based reasoning, rather than directly postulated. Several candidate mechanisms — including one in which the correct transition probability was inserted directly as a rule — were rejected on these grounds despite numerically reproducing the correct results, on the basis that a directly-postulated formula does not constitute a mechanistic explanation.

3. Research Methodology: A Collaborative Human-AI Approach

This research was conducted through extended, iterative dialogue between the author and Claude, an AI system developed by Anthropic, used throughout as a computational testing and verification partner rather than as an autonomous research generator. We report this methodology explicitly, as a relevant part of the scientific record, rather than treating it as an incidental detail of how the work was produced.

The working method was, in essence, a structured trial-and-error process, which the author characterised during development as analogous to a scattering experiment: a hypothesis about the underlying physical mechanism was proposed in plain physical language, translated into a precise numerical simulation, and tested immediately against the model's established sanity checks (same-setting invariance), its curve-fit accuracy against the quantum mechanical target, and, where relevant, the CHSH value. The result — whether confirming, refuting, or partially supporting the hypothesis — directly informed the next proposed variation. Across the course of this work, dozens of candidate mechanisms were proposed and tested in this manner; the substantial majority were rejected on the basis of failing one or more of these checks, and the specific manner of each failure was, in a number of cases, itself informative in narrowing the space of remaining candidates.

This process surfaced and corrected several genuine errors during development, which we consider worth reporting directly rather than omitting from the record. These included: an initial implementation in which a shared hidden variable was inadvertently constructed with a dependency on only one measurement setting, producing a CHSH value that briefly, and incorrectly, appeared to exceed the quantum mechanical maximum before the error was identified and corrected; a data-ordering bug in an early sequential-measurement implementation that produced a mathematically degenerate cancellation; a mislabelling of which measurement setting a given model parameter was weighted toward, discovered and corrected through direct numerical testing rather than assumption; and a trigger construction that selected the generative magnet using the same hidden spin label that also established the particles' anti-correlation at creation. This reproduced the correct transition curve and CHSH value under every check reported in Section 5, but was found, through explicit marginal-independence testing not otherwise required by those checks, to let one side's outcome statistics depend on the distant particle's measurement setting alone — a no-signaling violation. Decoupling the trigger from the spin label, so that it is instead a variable fixed at the particles' common origin but independent of either particle's later-measured spin, removed the dependency while reproducing every other reported result at the same precision (Section 5.2).

We regard the identification and correction of each of these errors as a genuine product of the iterative, adversarial character of the working method — in each case, a claim was made, immediately tested, found inconsistent with an established result, and revised — rather than as an incidental feature of using a computational tool.

We report this collaborative process transparently because we consider the resulting rate and structure of hypothesis testing — proposing a physical idea, obtaining a numerically verified answer within the same working session, and using that answer to constrain the next hypothesis — to be a material factor in the pace and scope of the investigation reported here, and one that the author judges would have been substantially more difficult to achieve at the same depth working without this iterative computational partnership.

4. Mechanistic Model

4.1 Core Variables

The model is built from four variables, tracked per particle. As established in Section 1, these are direct computational counterparts of the LGA framework's physical picture, not independently motivated abstractions:

- Particle_Angle — the particle's own orientation, corresponding to the neutron pulse's position on its figure-8 trajectory; a value in [0°, 360°), generated from a distribution concentrated around a relevant magnet's setting.
- Phase — a value cycling through a full 720° range rather than the ordinary 360°, corresponding to the dual-wave cycle described in Section 1.2, and reflecting the physical requirement that a spin-1/2 particle must undergo two full rotations to return to its original state.
- Spin — the measured outcome, read directly from Phase's position: Spin = (+) if Phase mod 720° < 360°, else Spin = (−).
- Magnet — the external measurement setting, a fixed angle in [0°, 360°).

The flip mechanism, applied identically in both the sequential and entangled cases, is defined as follows. Let rot = shortest_angular_path(Particle_Angle − Magnet), wrapped to the range (−180°, 180°]. If |rot| > 90°, a flip event occurs: Phase advances by exactly 360° (in the sign appropriate to the particle), and Particle_Angle itself is shifted by 180°, carrying this new orientation forward into any subsequent stage. This is the computational counterpart of the trajectory-lock transition described in Section 1.2 — the geometric consolidation that drives the pulse from its balanced double-loop path into a single-loop rotation. If |rot| ≤ 90°, no flip occurs and both variables remain unchanged.

4.1.1 The Wobble Distribution

Both the sequential pool (Section 4.2) and the entangled shared value (Section 4.3) are generated using a von Mises distribution — the standard circular analogue of a Gaussian, appropriate here because Particle_Angle is a circular quantity (0°-360°) rather than a linear one. Its probability density function is:

$$f(\theta; \mu, \kappa) = e^{\kappa \cdot \cos(\theta - \mu)} / (2\pi \cdot I_0(\kappa))$$

where μ is the mean direction (the relevant magnet's angle, in degrees, throughout this paper), κ is the concentration parameter, and $I_0(\kappa)$ is the modified Bessel function of the first kind, order zero. Larger κ corresponds to tighter concentration around μ, analogous to a smaller variance in a linear Gaussian. Throughout this paper, κ = 2.107, determined by the parameter search described in Section 5. A shared value is drawn by sampling from this distribution once, centred on the generative magnet's angle (Section 4.3) or on $Magnet_1$ (Section 4.2); resampling, where used, draws again from the same distribution, restricted to the subset of angles consistent with the required flip outcome (Sections 4.2 and 4.3).

4.1.2 Two Angular Degrees of Freedom

Although Particle_Angle is generated and stored as a single number, its role in the mechanism is better understood as two distinct angular coordinates on a sphere, in the ordinary physical sense of polar and equatorial (azimuthal) angles, each governed by a different rule.

The equatorial angle, φ, is Particle_Angle exactly as drawn from the von Mises distribution (Section 4.1.1). It is set once, at the moment of generation, and is not itself recalculated or rotated at any later step — it simply persists, unchanged, as a fixed value carried forward.

The polar angle, θ, is the quantity actually used in the flip threshold and torque comparison (Sections 3, 4): θ = shortest_path(Particle_Angle − Magnet). Because θ is defined relative to whichever magnet is currently measuring, the magnet's own direction serves as the polar axis. This has a direct and, on reflection, necessary geometric consequence for the torque derivation of Section 1.3: for the mirrored comparison $\tau\_magnetic(\theta)=\sin^2(\theta/2)$ against $\tau\_pulse(\theta)=\cos^2(\theta/2)$ to hold exactly, the crossover point (θ=180°, where flip is triggered) must sit precisely diametrically opposite the magnet's own direction (θ=0°) on this polar axis — which is exactly what the 180° Particle_Angle shift on flip (Section 3.1) implements.

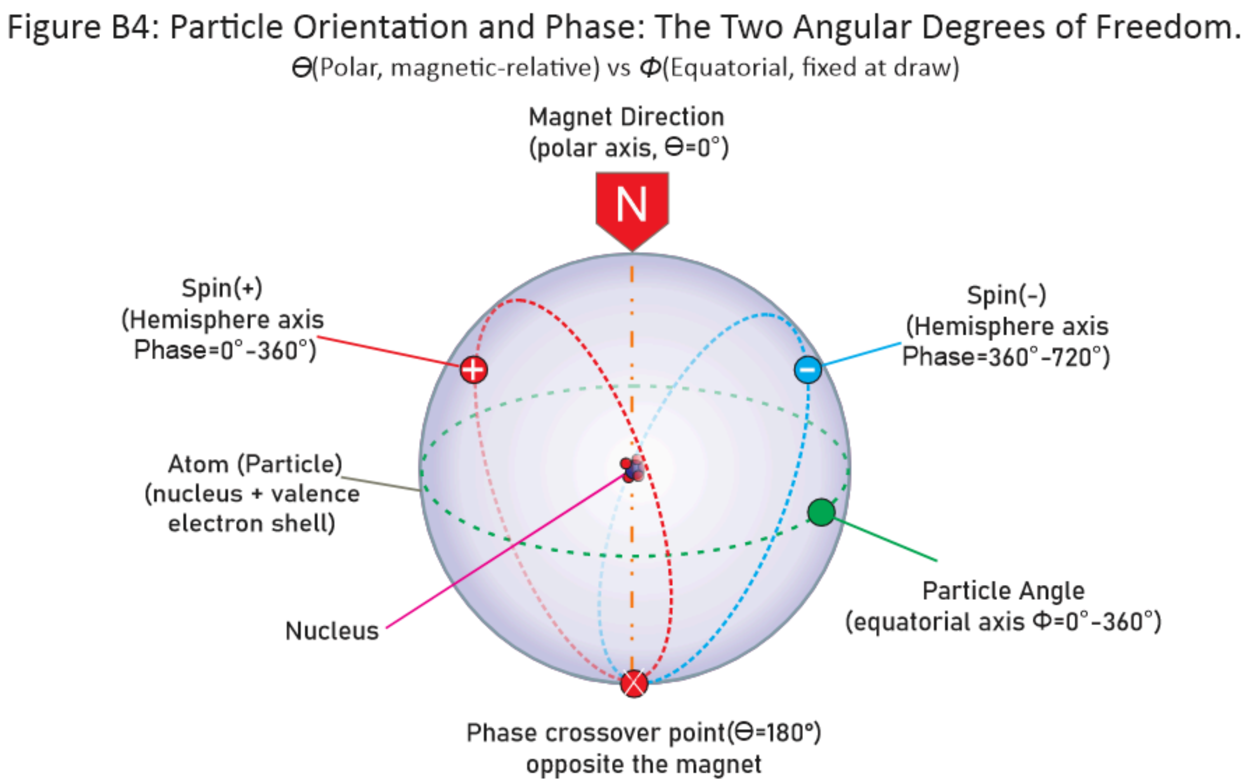

Figure B4. Particle Orientation and Phase: The Two Angular Degrees of Freedom. The atom — nucleus plus valence electron shell — sits at the sphere's centre. Spin(+) and Spin(−) correspond to the two halves of the electron's inherited 720° phase cycle (Section 1.2), occupying different planes in three dimensions; they meet at a single true crossing point at θ=180°, diametrically opposite the magnet. The equatorial angle φ (green) is fixed at the moment of generation.

This distinction clarifies a subtlety of the sequential mechanism (Section 4.2) worth stating explicitly: the equatorial angle φ can, and in the absence of a flip does, persist completely unchanged from Stage 1 to Stage 2 — yet the polar angle θ still differs between the two stages regardless, purely because it is measured against a different magnet each time. A single, unmoving equatorial value can therefore still yield genuinely different polar readings, and hence different measurement outcomes, at each stage.

4.2 Sequenced Single-Particle Mechanism

The sequential mechanism models one physical particle measured twice, at two magnet settings (Magnet$_1$, Magnet$_2$), applied in temporal order.

```
Pool = concentrated_distribution(center = Magnet₁, spread = 2.107)Particle_Angle(0) ~
Poolrot₁ = shortest_path(Particle_Angle(0) − Magnet₁)flip₁ = |rot₁| > 90°Result₁ =
−initial_state  if flip₁,  else  initial_stateParticle_Angle(1) ~ resample(Pool, Magnet₁,
conditioned on flip₁)rot₂ = shortest_path(Particle_Angle(1) − Magnet₂)flip₂ = |rot₂| >
90°Result₂ = −initial_state  if flip₂,  else  initial_stateOutcome: Same if Result₁ =
Result₂, else Different
```

A critical structural requirement, confirmed only after extensive testing of alternatives, is that Result$_2$ must be computed fresh from the original initial_state, rather than by applying flip$_2$ cumulatively on top of Result$_1$. Formulations that stacked the two flip events produced a mathematically degenerate cancellation (two flips returning the particle to its original, unflipped classification) and failed to reproduce the correct curve.

Figure 4: Sequenced Single-Particle Mechanism

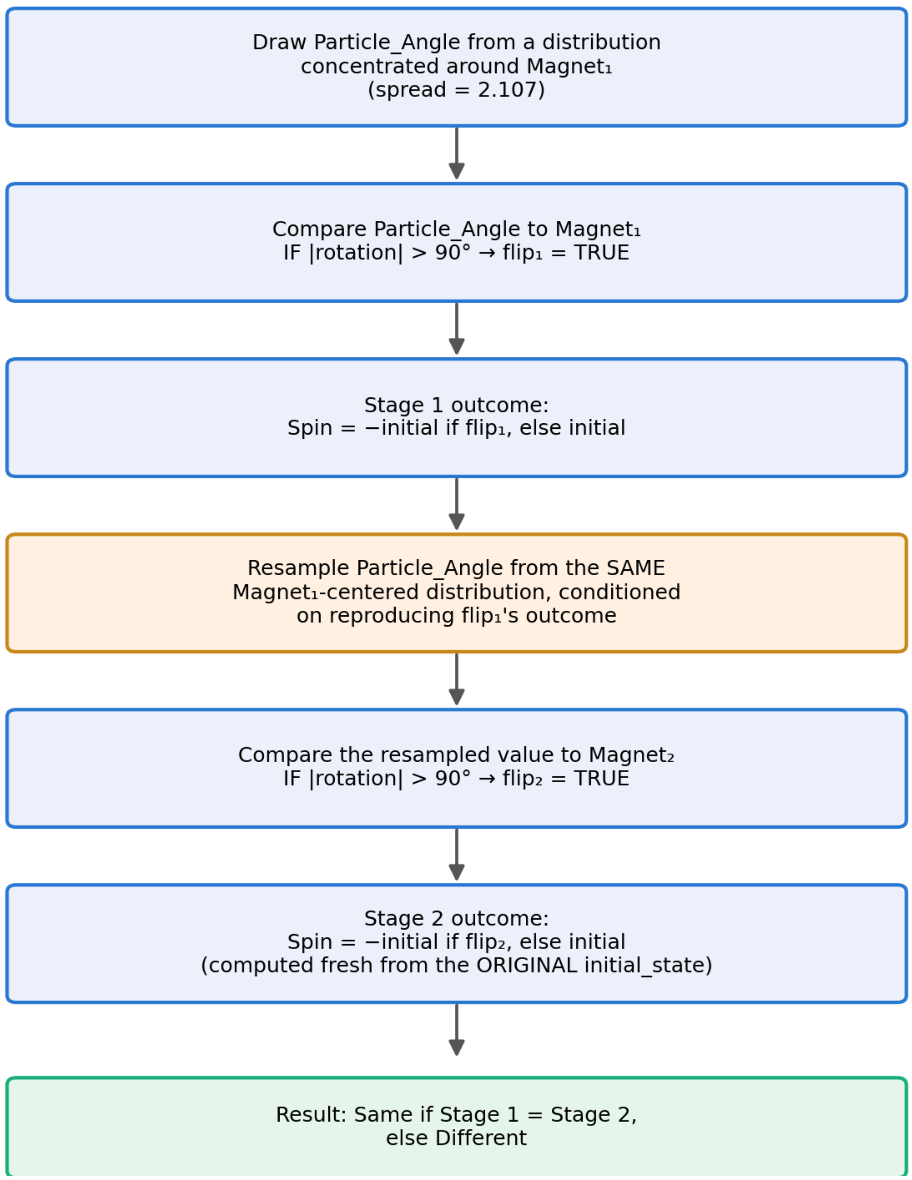

Figure 4. Flow diagram of the sequenced single-particle mechanism. The shaded step (resampling) represents the physical claim, established in Section 1.2, that measurement genuinely disturbs the particle's trajectory, not merely its recorded label.

Two fully worked examples of Figure 4 are given below: one producing a 'Same' outcome with no flip at either stage, and one producing a 'Different' outcome via a single flip at the second stage.

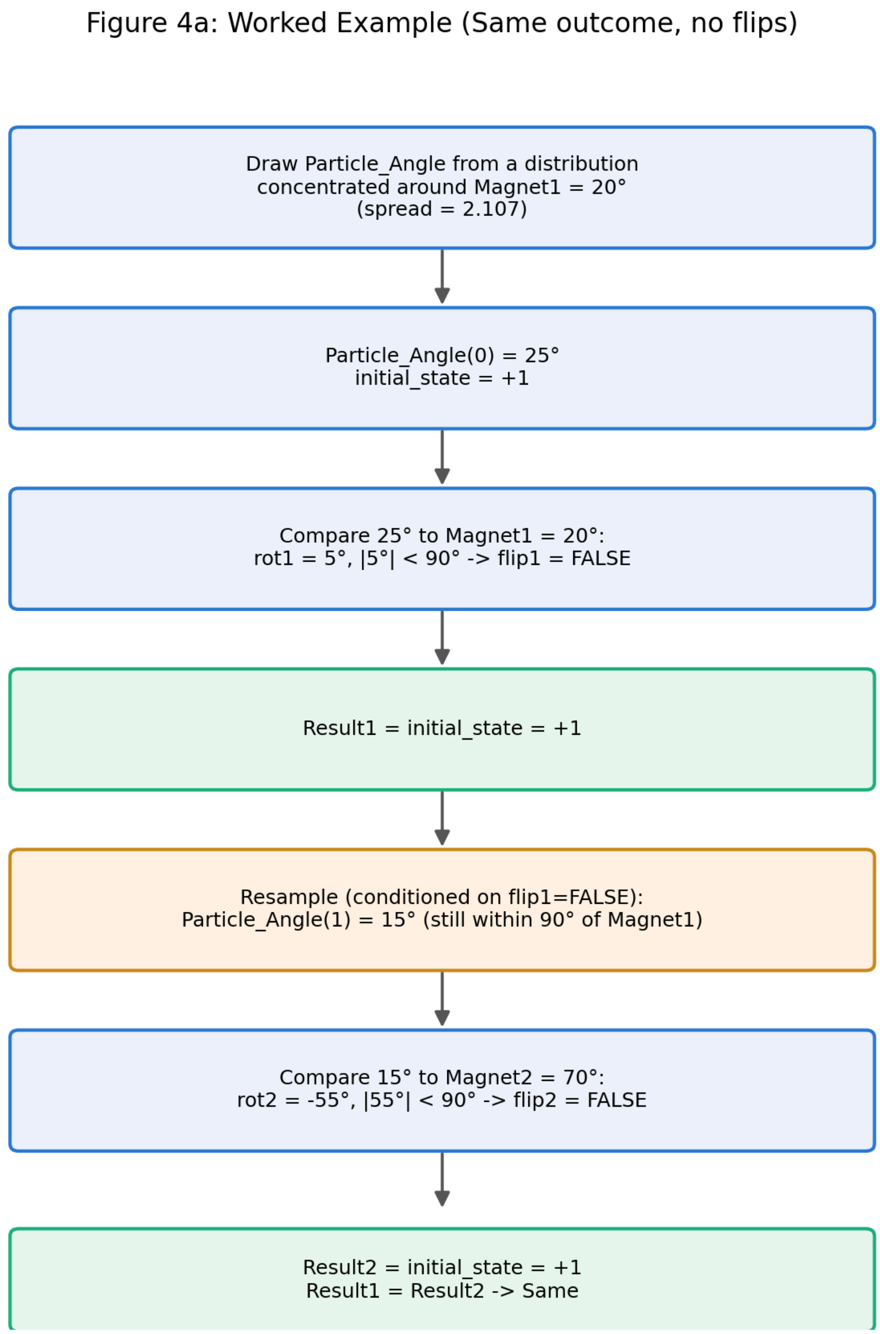

Figure 4a. Worked example of a 'Same' outcome. The particle starts and remains within 90° of Magnet1 at both the initial draw and the resampled value, and this same resampled value also falls within 90° of Magnet2, so neither stage flips and the two results agree.

Figure 4b: Worked Example (Different outcome, via a flip)

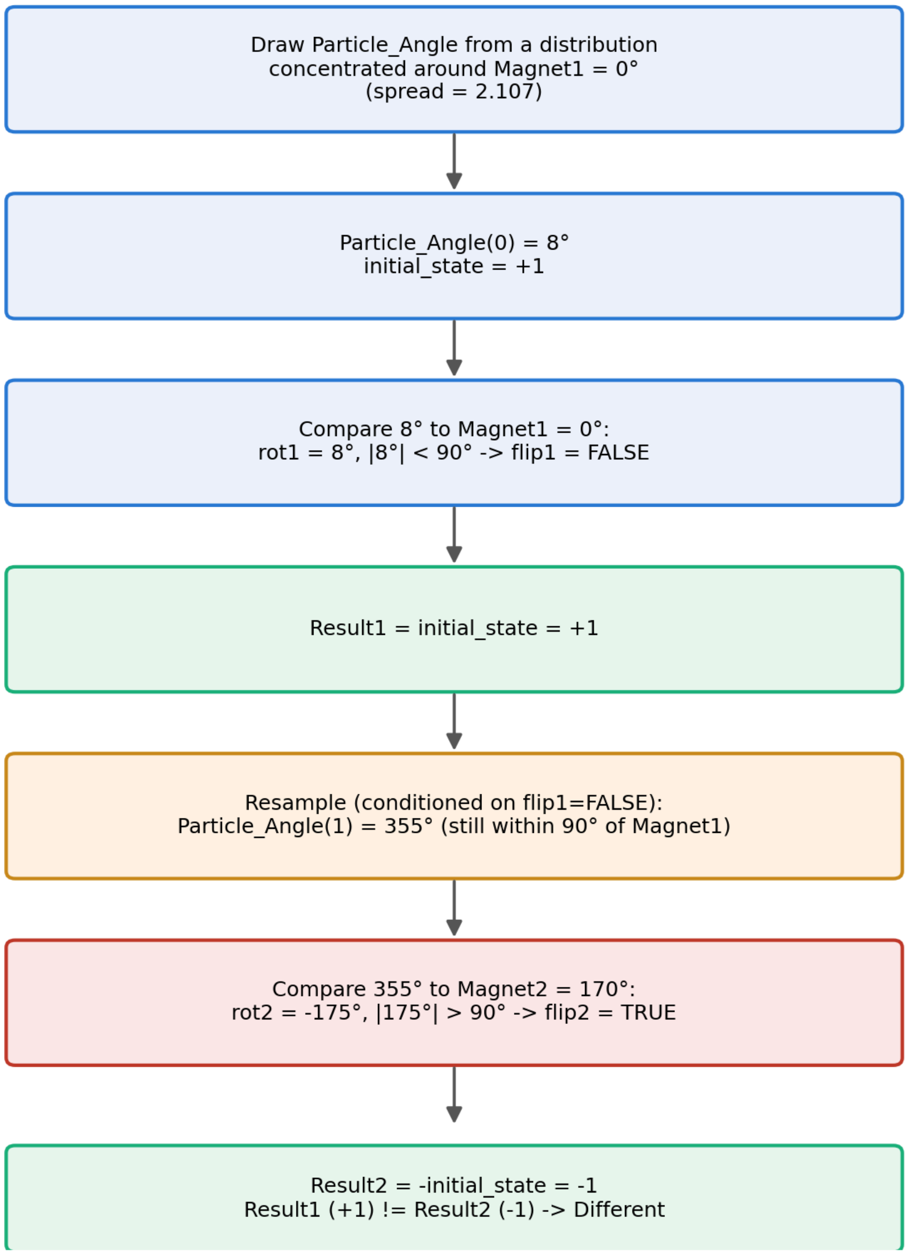

Figure 4b. Worked example of a 'Different' outcome via a flip. The first stage does not flip, but the resampled value happens to fall more than 90° from Magnet2, triggering a flip at the second stage and reversing the result relative to Stage 1.

4.3 Entangled Pair Mechanism

The entangled mechanism extends the same building blocks to two spatially separated particles, sharing a common origin, consistent with the phase-locked pulse pairs described in Section 1 as the LGA account of entanglement.

Which particle's magnet is generative is decided by an origin-fixed trigger variable, established at the same moment as the particles' anti-correlated spin labels but drawn independently of them.

```
initial_A = random(+1, −1);  initial_B = −initial_Aorigin_trigger = random(0, 1)   --independent of initial_ATrigger: IF origin_trigger = 0 THEN generative_magnet = Magnet_A ELSE                      generative_magnet = Magnet_BShared_Particle = generative_magnet + wobble(spread = 2.107)rot_A = shortest_path(Shared_Particle − Magnet_A); flip_A = |rot_A| > 90rot_B = shortest_path(Shared_Particle − Magnet_B); flip_B = |rot_B| > 90Spin_A = −initial_A if flip_A else initial_ASpin_B = −initial_B if flip_B else initial_BOutcome: Different if Spin_A ≠ Spin_B, else Same
```

In plain terms:

At creation, the two particles' phase-locked trajectories are established as mirror images of one another — one destined to read Spin(+), the other Spin(−) — and, independently, an origin-fixed coin designates one of the two magnets as generative.

The particle on the generative side orients directly and exclusively to its own magnet, with a small amount of natural wobble, and has no dependence on the other particle's magnet at all.

The other particle does not undergo its own trajectory-orientation process — it inherits the already-oriented trajectory value that the generative side produced.

Each particle's magnet then performs a reading of this shared trajectory value using only its own setting, exactly as in the sequential case; the non-generative magnet never contributes to shaping the trajectory, only to measuring it.

Reduced form. Since only the generative magnet contributes to the shared value's generation, the mechanism can be restated using a single magnet angle at the generative stage:

```
Shared_Particle = Magnet_[generative] + wobble(spread = 2.107)
```

with the other magnet entering the calculation only afterward, as a passive reference angle used solely to read a threshold comparison against an already-complete value. We regard this distinction — one angle that participates in generating the shared state, one that only measures it, decided by a variable independent of either particle's own eventual spin — as the central structural finding of this work, and discuss its interpretation in Section 6.

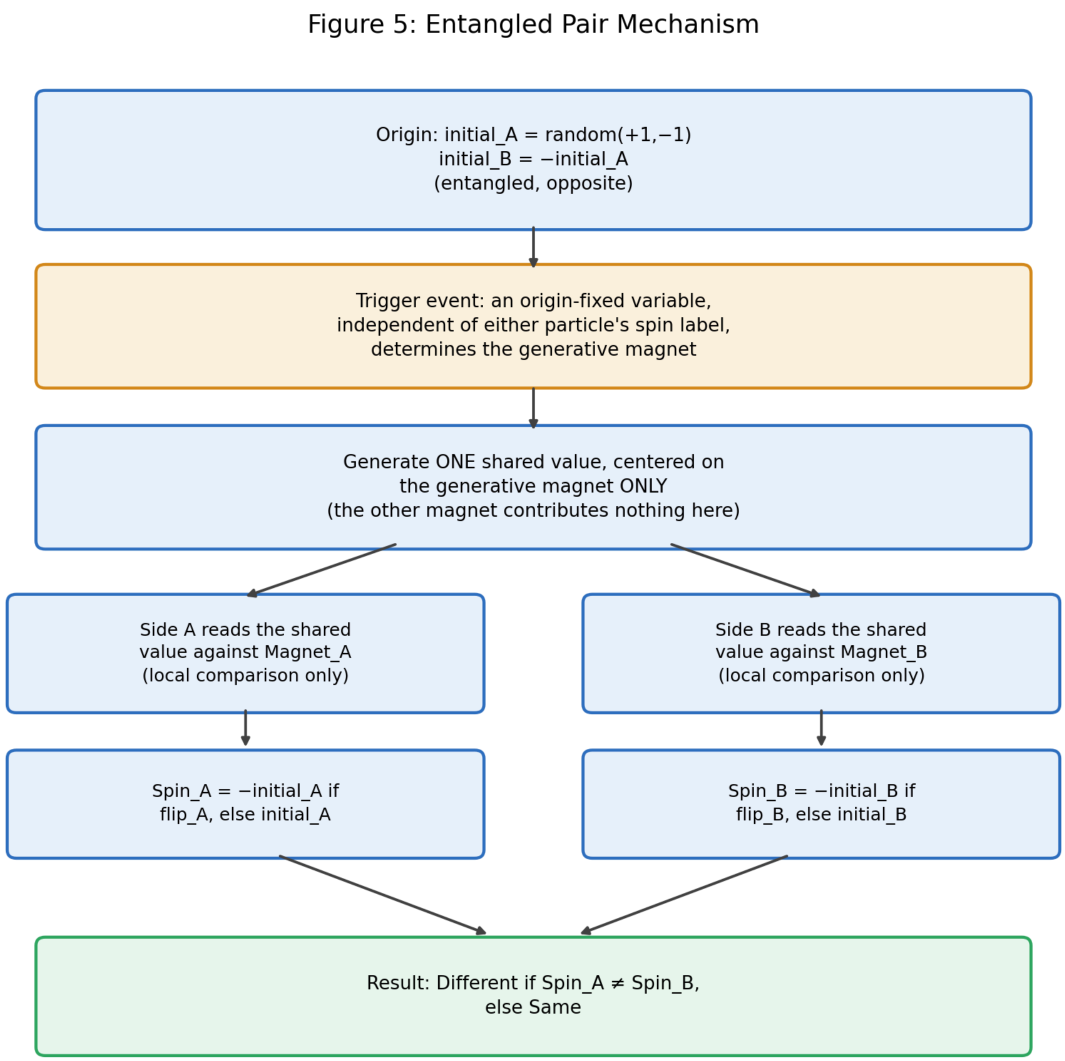

Figure 5. Flow diagram of the entangled-pair mechanism. The trigger event (orange) is fixed at the particles' common origin and independent of either particle's spin label; four operationally distinct physical stories for it were tested and found numerically indistinguishable, provided each is genuinely independent of spin label (Section 6.3).

Two fully worked examples of Figure 5 are given below: one producing a 'Different' outcome without any flip event, and one producing a 'Same' outcome via a single flip on one side, illustrating that the two particles' final agreement or disagreement depends on how each side's own magnet happens to relate to the one shared value, not on any direct comparison between the two magnets themselves.

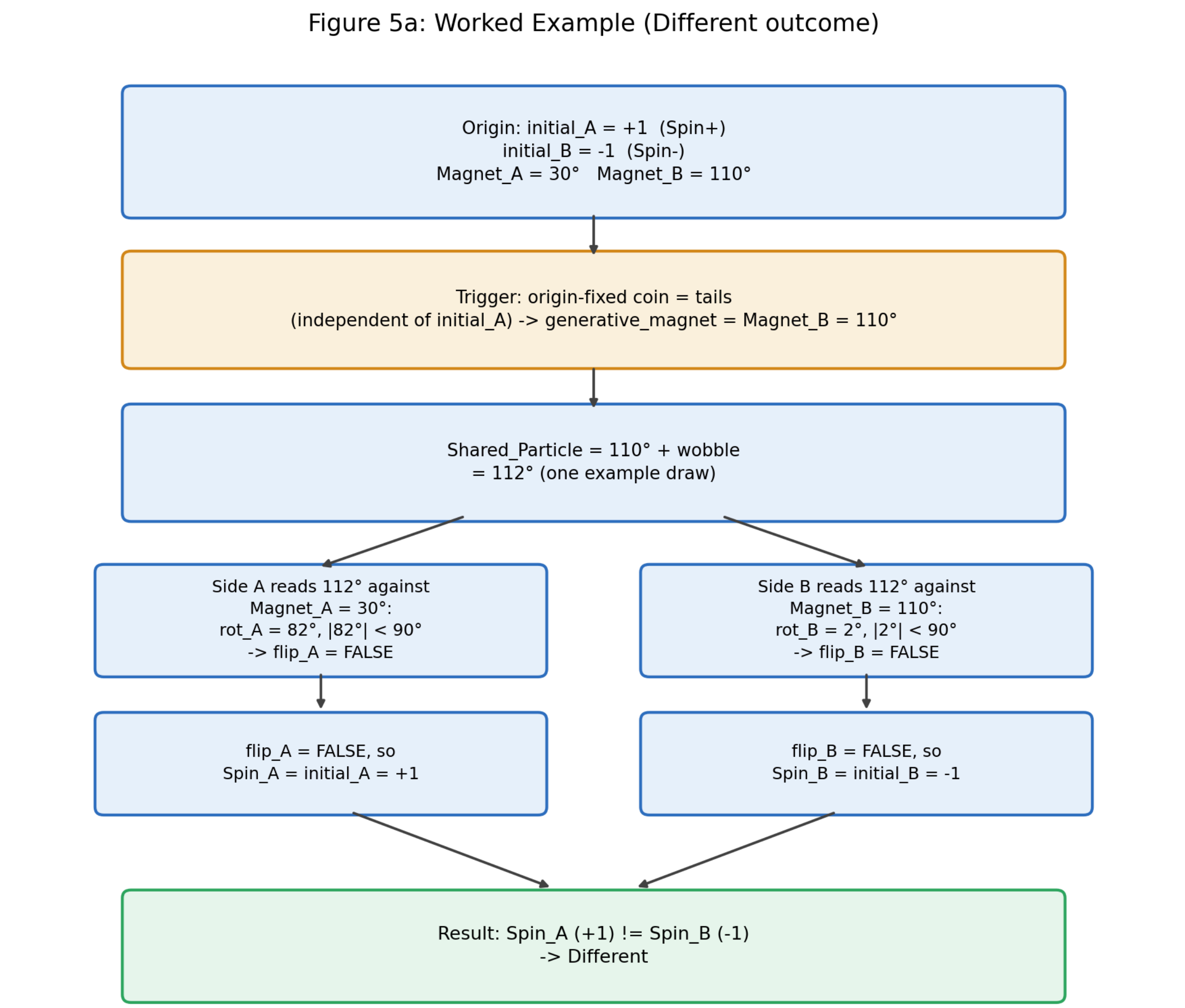

Figure 5a. Worked example of a 'Different' outcome. The origin-fixed trigger selects Magnet_B (110°) as generative; the shared value (112°) lies within 90° of both magnets, so neither side flips, and the particles retain their original, opposite labels.

Figure 5b: Worked Example (Same outcome, via a flip)

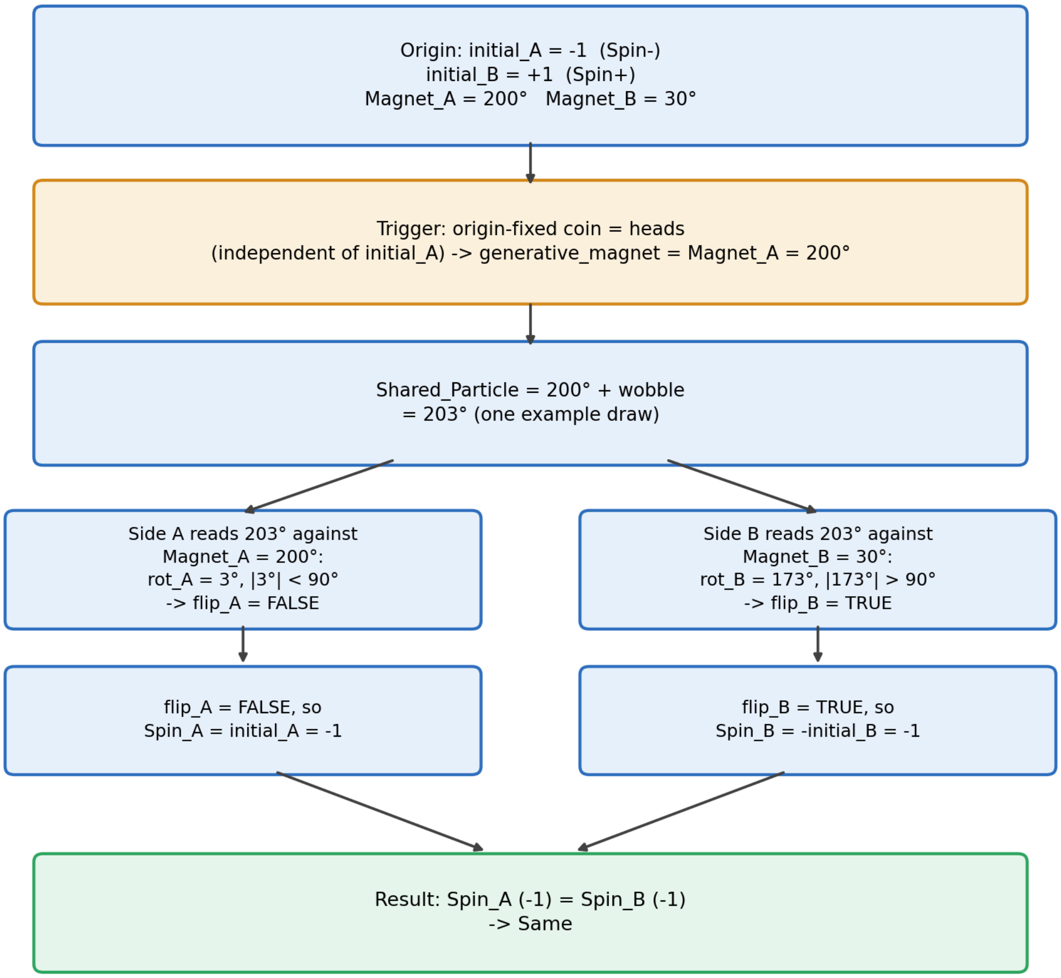

Figure 5b. Worked example of a 'Same' outcome via a flip. The origin-fixed trigger selects Magnet_A (200°) as generative; the shared value (203°) lies more than 90° from Magnet_B (30°), triggering a flip on side B that reverses Spin_B and brings the two particles into agreement.

5. Results

5.1 Sequential Single-Particle Results

Same-setting invariance ($Magnet_1 = Magnet_2$) was verified at five angles, sample size 100,000 trials per angle, with all results returning exactly 100.0% 'Same', consistent with the deterministic-repeat-measurement result required by quantum mechanics.

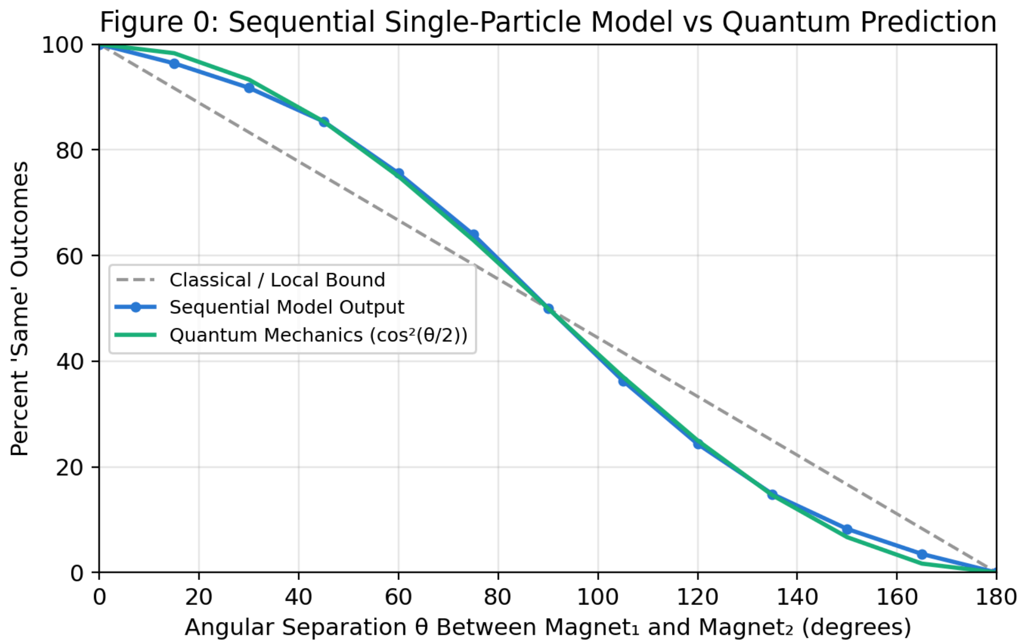

Figure 0. Sequential model output (blue) closely tracks the quantum mechanical transition probability $\cos^2(\theta/2)$ (green) across the full separation range, with a maximum deviation of approximately 1.6 percentage points.

Rotational consistency (fixed 45° separation, varying starting reference angle) was verified across five reference angles, returning results clustered between 85.14% and 85.36%, against a constant quantum target of 85.36%.

Three-stage measurement disturbance. A classic result in quantum measurement theory holds that an intervening measurement along an axis incompatible with the first erases the information carried by that first measurement: a particle measured 'up' along axis Z, then measured along an unrelated axis X, will show a fully random (50%) result if measured along axis Z a third time — rather than deterministically reproducing 'up', despite having already been established as 'up' by the first measurement. This corresponds directly to the field-competition and trajectory-lock account of Section 1.2: the intervening X-axis field genuinely re-settles the trajectory, rather than leaving the particle's prior Z-axis lock undisturbed.

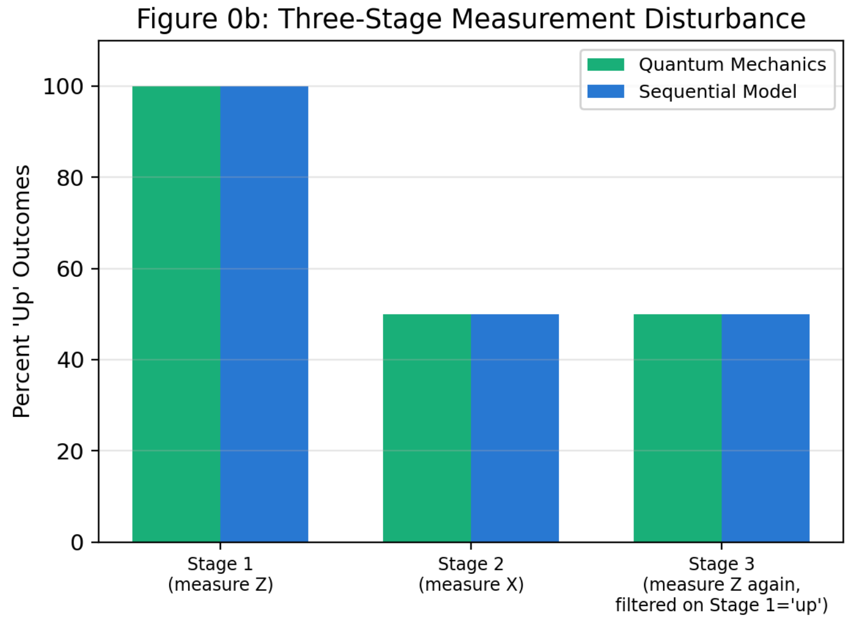

Figure 0b. The model correctly reproduces the disturbance effect: despite all filtered particles having previously measured 'up' along Z, the intervening X measurement reduces the third-stage Z result to 49.9%, closely matching the quantum mechanical prediction of exactly 50%, and sharply distinct from the 100% that would result if the first measurement's information had persisted undisturbed.

5.2 Entangled Pair Results

Same-setting invariance was verified at eight angles spanning the full 360° range, sample size 150,000 trials per angle, with all results returning exactly 100.000% 'Different' (the singlet-state anti-correlation required at zero separation).

The full correlation curve was computed across the 0-180° separation range and compared against $\cos^2(\theta/2)$.

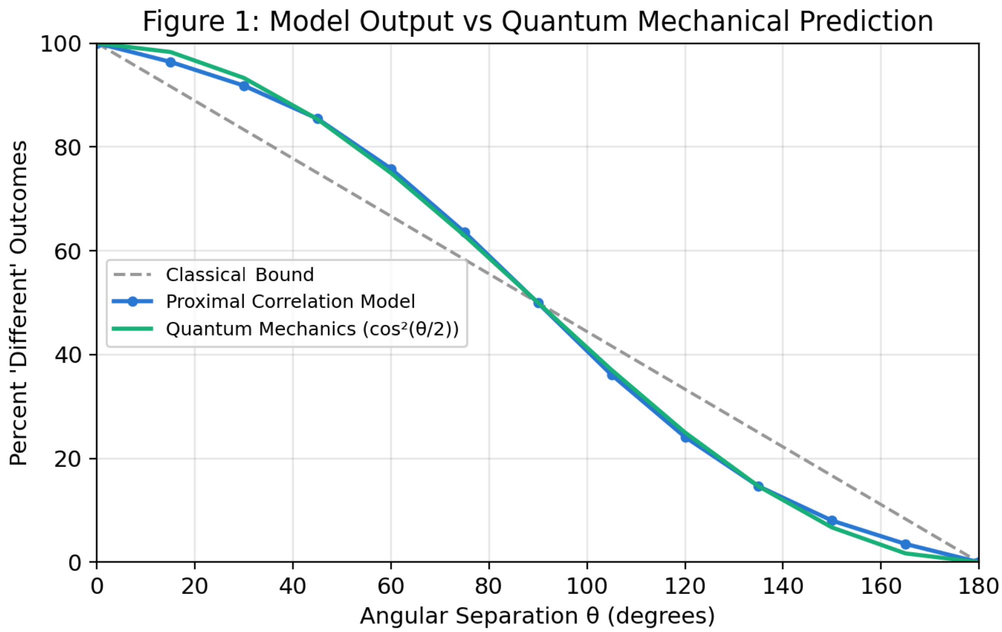

Figure 1. Model output (blue) closely tracks the quantum mechanical prediction (green) and diverges substantially from the classical linear bound (grey dashed) that any model with fully independent, per-particle inputs is restricted to. Maximum deviation across the sweep: 1.9 percentage points.

Rotational consistency (fixed 45° separation) was verified across five starting reference angles: 85.10–85.22%, against a constant quantum target of 85.36%.

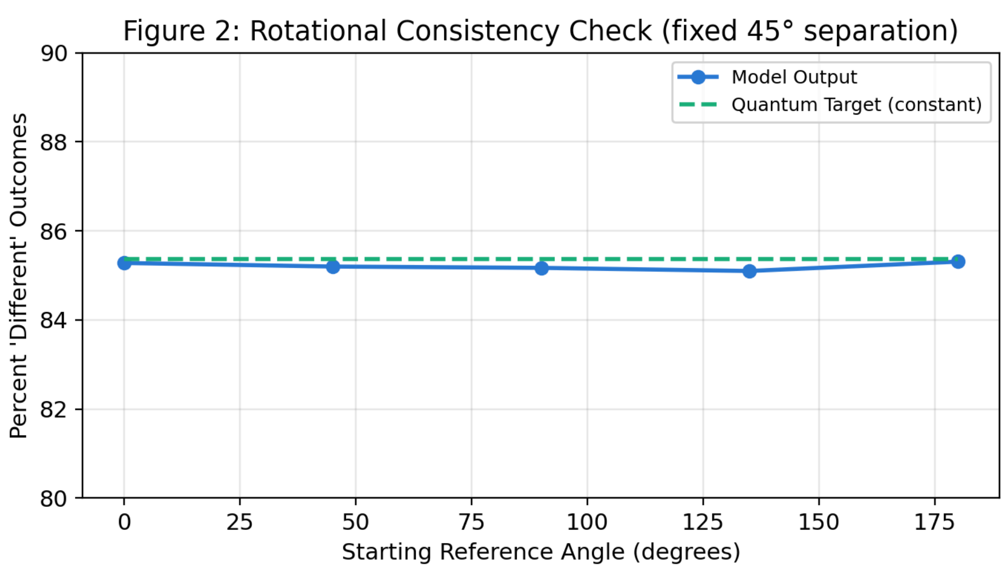

Figure 2. The model's output for a fixed 45° separation remains tightly clustered regardless of the absolute starting angle, closely matching the constant quantum target of 85.36%. Earlier iterations of this mechanism, using a fixed-shape density anchored to absolute angular reference points, showed substantial inconsistency (a swing of up to 18 percentage points) under this same test; see Section 6.4.

The four correlation terms required for the CHSH combination were computed at the conventional optimal test angles (a=0°, a'=90°, b=45°, b'=135°), sample size 300,000 trials per term.

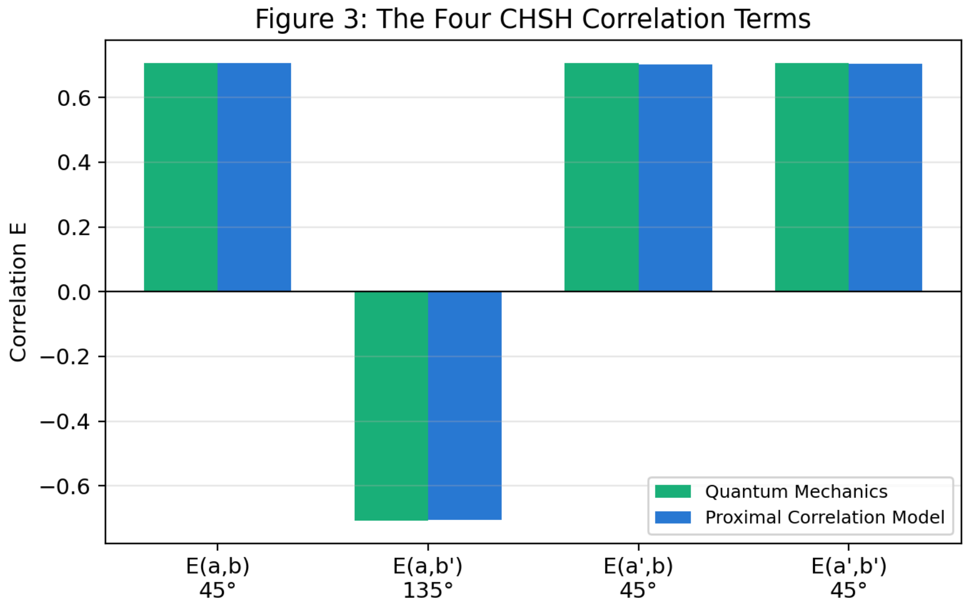

Figure 3. The model reproduces both the magnitude and, critically, the sign pattern of the four quantum correlation terms — the E(a,b') term correctly inverts relative to the other three, which is the structural feature responsible for constructive rather than destructive combination in the CHSH sum.

S = E(a,b) − E(a,b') + E(a',b) + E(a',b') ≈ 2.818, exceeding the classical bound of |S| ≤ 2.0000 — the maximum reachable by any model in which each particle's outcome depends only on its own local setting — and closing to within 0.4% of the quantum mechanical maximum of 2√2 ≈ 2.8284.

5.2.1 Marginal Independence (No-Signaling)

Because the origin-fixed trigger never references either particle's spin label, one side's unconditioned outcome statistics should be entirely independent of the other side's chosen measurement setting — a basic requirement of any physically consistent account of entanglement, and one distinct from, and more fundamental than, the CHSH bound itself. This was tested directly: holding one side's magnet fixed and sweeping the other's setting across the full 0–360° range (20° steps, 150,000 trials per point) changed the held side's marginal ('% up', ignoring the distant side's results entirely) by no more than 0.5 percentage points in either direction — consistent with statistical noise at this sample size, and confirming the mechanism does not permit one party to detect the other's setting from their own statistics alone. We report this check explicitly because it is not implied by same-setting invariance or the CHSH value alone (Section 6.1), and because an earlier trigger construction that appeared to pass every other check in this section failed it (Section 3).

5.3 On the Relationship Between Curve-Fit Accuracy and the Shared-Value Structure

Because both the sequential and entangled mechanisms reproduce the same $\cos^2(\theta/2)$-shaped curve to comparable accuracy (Sections 5.1 and 5.2), it is important to be precise about what this shared result does, and does not, establish about the underlying dependency structure. Curve-fit accuracy alone does not distinguish a model in which each side's outcome depends only on its own setting from one in which the two sides' outcomes are tied to a shared value: both kinds of process can, in principle, produce the same distribution of 'same' versus 'different' outcomes as a function of angular separation, since this curve describes only the frequency of outcomes at a given separation, not the specific cross-dependency structure that produces them.

The CHSH value S, by contrast, is sensitive to exactly this structure, because its construction requires combining correlations across four distinct pairings of two independently-chosen settings (Section 5.2) — a combination that is only definable, and only meaningful, for a genuinely two-party, two-setting system. The sequential mechanism, involving a single particle and no second, independently-set observer, has no shared-value alternative to be compared against in the first place — there is only one particle, so the question of whether its outcome depends on a second setting does not arise. The entangled mechanism's dependency structure, by contrast, is established specifically by its S value and its marginal-independence result (Sections 5.2, 5.2.1), not by its curve fit. We report all three together in this paper because they arise from directly related mechanisms and because their similarity is itself informative — but we emphasise that matching the curve is a necessary, not a sufficient, condition for establishing that structure, and that S and marginal independence remain the determining tests, applicable only to the two-particle case.

6. The Proximal Correlation Model

6.1 Locating the Shared-Value Step

A direct test was performed to determine whether the entangled mechanism could be restructured so that each particle's process referenced only its own magnet, with no shared dependency at all. Two independent attempts — a version in which the two particles drew entirely independent random values, and a version in which they shared only a neutral, magnet-independent origin value before each independently 'aligning' to its own field — both failed the same-setting invariance test outright (reducing to approximately 50%, rather than the required 100%). We take this as a direct, mechanistic demonstration, rather than a purely formal one, that some form of shared dependency between the two particles' final states is structurally necessary for the model to function at all, and is not an avoidable simplification. We further tested whether the second magnet could contribute even a small, independent influence to the shared value without disturbing this result: introducing an additional pull toward the second magnet's setting, at a weight as small as two percent, was sufficient to degrade same-setting invariance measurably below the required exact value. We take this as confirmation that the mechanism's structure is not one of degree — the second magnet's setting must play no generative role whatsoever, rather than a merely small one, for the model to remain internally consistent.

Systematic testing located this dependency to a single, minimal point: the generation of the one shared Particle_Angle value requires access to the eventual measurement setting of exactly one of the two magnets (Section 4.3), designated by a trigger variable fixed at the particles' common origin and independent of either particle's own spin label or later-measured outcome. The other magnet's setting is never referenced during this generative step, entering the calculation only afterward, in a threshold comparison that uses only its own setting. This is, to our knowledge, a more constrained and specific dependency than is typically described in the hidden-variable literature, where dependency on both settings, or a general disturbance of the hidden-variable distribution, is more commonly proposed (see Section 6.5).

6.1.1 Why Distance Does Not Exempt the Generative Magnet

A natural objection to the mechanism described above is that the generative magnet may be physically distant from the particle pair's point of origin, and that magnetic field strength is well known to fall with distance. We note that this objection conflates field strength with orientation outcome. A compass needle in a very weak magnetic field does not settle into a partially-aligned or ambiguous orientation; given sufficient time and the absence of an interfering, comparably-strong local field, it still orients fully toward magnetic north. Field strength governs the rate and torque of the orienting process, not its eventual outcome. On this basis, we take it as physically reasonable that a distant generative magnet can still fully determine the shared value's orientation at the point of origin, provided no stronger, intervening magnetic source is present to compete with it, independent of the specific distance involved.

A related but distinct question is what happens when both magnetic fields are simultaneously present at the particles' point of origin — as, physically, they must be, since both magnets' fields propagate outward from the moment their angles are set (Section 6.1.2) and neither field's presence can simply be switched off. The answer is not that the particle settles into some intermediate compromise, partially aligned with each field in proportion to their relative strengths. A system balanced between two competing influences of this kind is analogous to a ball balanced on the point of a needle, or to an ordinary magnet's own spontaneous magnetization: at the moment its state is fixed, the outcome is not a blend but a clean choice of one direction over the other, because a partially-committed state simply is not a stable configuration. This is not merely a convenient assumption; it is what the direct numerical test reported in Section 6.1 already found — introducing even a 2% weighted contribution from the second magnet was sufficient to measurably break the model's otherwise-exact same-setting invariance. The trigger described in Section 6.1.2 is best understood as supplying the answer to which direction such a system resolves toward — the same role played by whatever microscopic asymmetry decides which way a balanced needle actually falls — rather than as an additional, independently-motivated ingredient bolted onto the physics.

6.1.2 The Moment of Information Transfer

It is worth stating precisely, in physical rather than purely computational terms, the full sequence of events by which the generative magnet's setting is imprinted onto the passive particle, since this is the process responsible for the shared-value dependency identified above. We set this out here as a six-step causal chain, illustrated in Figure B3, extending the two-step account given in earlier drafts of this paper to make explicit the physical role of both magnets' fields and the timing of each event.

Step 1 — Fields propagate. The two magnets are set to their respective angles, and their magnetic fields propagate outward from that moment, at a speed no greater than that of light, filling the surrounding region — including, in time, the point at which the entangled particle pair will be created.

Step 2 — Both fields reach the origin. The particle pair is created at a point already within reach of both magnetic fields, however weak either field's strength may be at that location. Both fields are genuinely present; as established in Section 6.1.1, this does not mean either field can lend the particle a partial, blended orientation.

Step 3 — One particle orients, fully. An origin-fixed trigger — independent of either particle's eventual spin label (Section 6.3) — designates one of the two particles as the one whose orientation is generated first, toward its own (favoured) magnet. Because the two fields cannot produce a stable, partially-aligned outcome (Section 6.1.1), this particle's angular position locks fully onto the favoured magnet's direction; the other field's presence, though real, contributes nothing to this outcome. This is an ordinary, local orienting event, no different in kind from a compass needle settling toward magnetic north.

Step 4 — The other particle mirrors it. The second particle does not independently orient to any magnet. Through the spin-coupling that established the pair's anti-correlation at creation, it instead inherits the same angular value the first particle generated. This is the mirroring event described in earlier drafts of this paper, and remains the specific step responsible for carrying the generative magnet's influence to the second particle.

Step 5 — The particles separate and travel. The two particles travel apart, each carrying this one shared angular value, unchanged, toward its own respective magnet.

Step 6 — Each magnet reads its own particle. At each magnet, the arriving particle's carried angular value is compared against that magnet's own setting. If the angular separation exceeds 90°, the spin reads as flipped relative to the particle's initial label; otherwise it reads as unflipped (Section 4.1). Because the shared value was generated centred on only one magnet's setting, the favoured particle's own comparison rarely flips; the second particle's comparison, against a potentially quite different magnet, is a separate, one-time check with no relation to what happened during Steps 3–4.

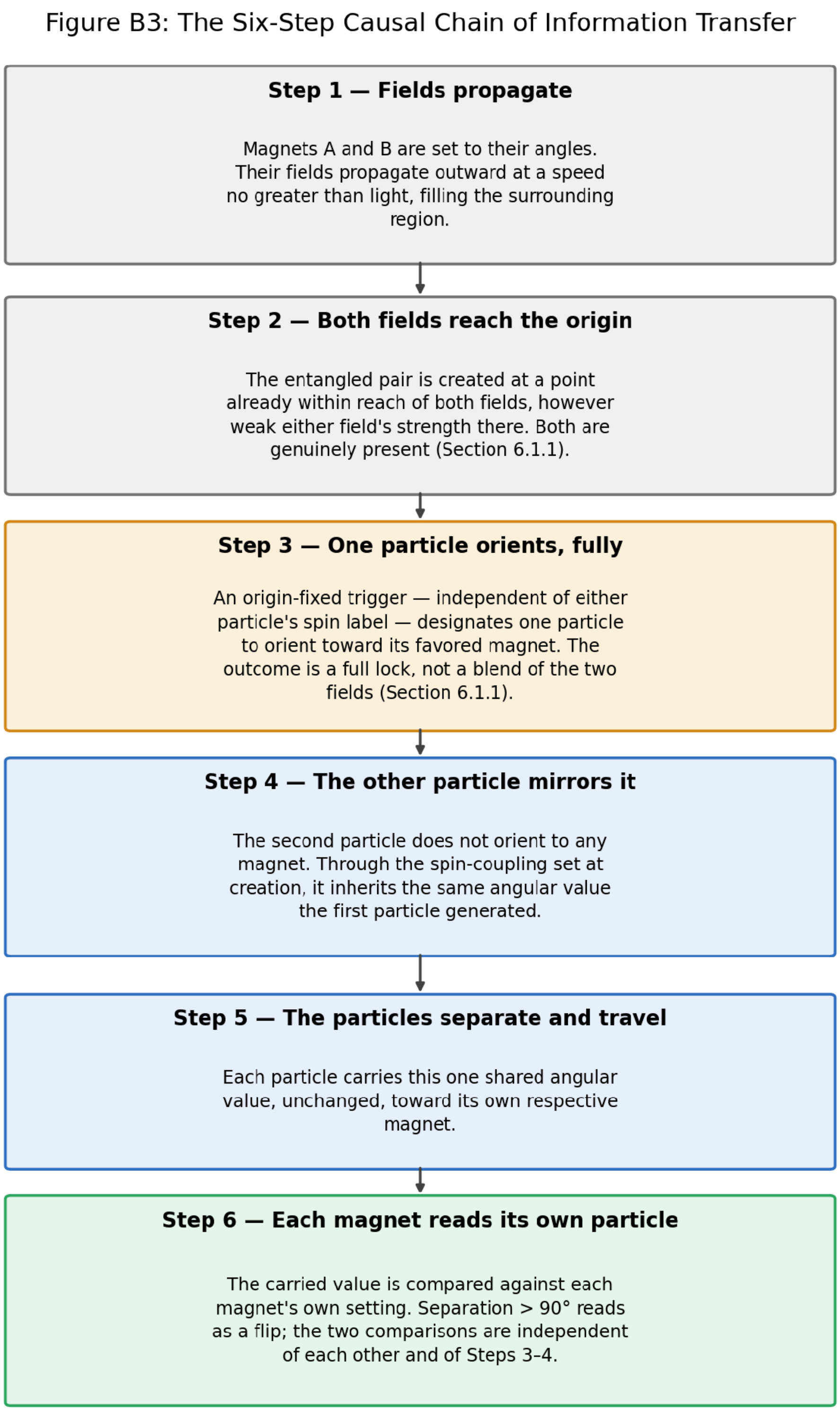

Figure B3. The six-step causal chain of information transfer. Both magnets' fields are physically present at the origin from Step 2 onward, but only the favoured magnet participates in Step 3's orientation event (Section 6.1.1); the other particle's mirroring (Step 4) and each side's independent measurement (Step 6) complete the chain. Which particle is favoured is fixed at the origin, independent of either particle's spin label.

This can be restated more precisely using the polar/equatorial distinction introduced in Section 4.1.2. The shared value φ is drawn from a distribution centred on the generative magnet (Step 3) and is therefore already polar-aligned to that magnet's own direction from the moment of its generation, before the other magnet is consulted at all. When the other side subsequently computes its own polar angle, θ = shortest_path(φ − Magnet), using only its own setting and this one shared φ (Step 6), the result is nevertheless shaped by the generative magnet's setting indirectly, because φ itself already carries that imprint by construction. The non-generative side's calculation, in this precise sense, uses only its own setting — it never references the generative magnet's angle directly — yet its outcome is not independent of it, because the one shared quantity it operates on was never generated independently of it to begin with.

6.2 Causal Consistency Under a Fixed-Prior-to-Separation Assumption

The model as constructed is causally consistent provided both measurement settings are established prior to the physical separation of the two particles. Under this assumption, the information required to generate the shared value — the angle of the generative magnet — is co-located with the particle pair at a single point in spacetime, and no signal is required to travel between separated locations, at any speed, to construct the model's output.

We explicitly distinguish this from a scenario in which either measurement setting is chosen or altered after the particles have separated. Under that scenario, and using the mechanism as described, the shared-value generation step would require information about a setting decided at a spacelike-separated location, which — depending on the precise timing — could require superluminal transfer of information to satisfy. This scenario was not tested in the present work; we regard it as outside the scope of a model developed and validated under the fixed-prior-to-separation assumption, and suggest that photon-polarizer experiments, which have directly tested delayed and in-flight setting changes (Aspect, Grangier, & Roger, 1982), are a more appropriate point of comparison for that specific question.

This boundary is worth stating plainly rather than resolving. Within the atomic, magnet-based system studied throughout this paper, reproducing the reported correlations does not require anything beyond the specific, identifiable event described in Section 6.1, provided the fixed-prior-to-separation assumption holds. We tested directly what happens when that assumption is relaxed — settings chosen only after the particles separate, as delayed-choice experiments are specifically designed to require — using constructions in which the shared value cannot reference either setting, since neither exists yet at the moment it must be generated; every such construction we tried reduced exactly to the classical bound of 2 (Section 8), consistent with Bell's theorem. This is, at present, an internal consistency result only: no experimental test of entangled atoms measured with magnets under genuine delayed choice exists to compare it against, so there is nothing yet for this result to be checked against. The analogous question for photon polarization — a physically distinct system, with its own geometry, not yet studied in this line of work — remains open, and we draw no conclusion from the atomic case about how it will resolve.

6.3 Equivalence of Candidate Trigger Mechanisms

Several operationally distinct physical stories can be told for what fixes the trigger at the particles' common origin: an auxiliary random event at creation, the relative order in which the two measurements are later completed, proximity of an auxiliary random draw to each magnet, or a distance-like variable. Provided each is genuinely independent of the particles' own spin labels — a condition spin label itself, by construction, cannot satisfy — these produce statistically indistinguishable results (S = 2.815 to 2.823 across variants tested). We report this as an honest limitation rather than a result: as constructed, each of these triggers reduces mathematically to an unbiased binary choice, and the present body of numerical testing cannot distinguish between them. A trigger mechanism that produced differing predictions under some testable condition would be required to adjudicate between these physical interpretations.

We note the boundary of this equivalence class explicitly: any candidate trigger that is itself correlated with either particle's later-measured outcome — spin label being the clearest example — reintroduces the marginal dependency identified in Section 5.2.1, regardless of its physical story. The equivalence reported above holds only among triggers satisfying this independence condition.

6.4 Density Shape and Rotational Consistency

An earlier iteration of this model generated the shared particle value from a fixed-shape density (an asymmetric, tip-and-crossing-weighted profile, independent of which magnet was being measured) rather than a density dynamically concentrated on the relevant magnet at the time of generation. This earlier version reproduced the correlation curve accurately when tested from a single, fixed absolute reference angle, but failed the rotational consistency test described in Section 5.2, with deviations of up to 18 percentage points depending on the starting angle. We take this as a clear demonstration that a physically adequate model must generate its density dynamically, relative to the actual measurement context, rather than from a density fixed to absolute spatial orientation — and note this as a specific, falsifiable design constraint for any related model.

6.5 Relation to Existing Categories

We distinguish the Proximal Correlation Model from three established categories in the hidden-variable literature:

- Superdeterminism proposes that the experimenter's choice of measurement setting is correlated with the particle's state via a common cause tracing to the origin of the universe. The present model requires no such cosmological pre-correlation: the dependency is established at a specific, identifiable physical event (the particles' shared point of origin, prior to separation) and remains fully causal under that assumption.
- Bohmian mechanics (Bohm, 1952) achieves the full quantum correlation via a continuously-existing guiding field that updates instantaneously in response to the complete experimental configuration. The present model requires no continuous field; the dependency is fixed once, at a single generative event, and is not subsequently updated.
- Retrocausal models propose that a later measurement choice influences the particle's earlier state via backward-in-time influence. The present model, under the fixed-prior-to-separation assumption of Section 6.2, requires no backward-in-time influence at all.

We also compared the present approach directly against a published local hidden-variable model (Matzkin, 2007), which similarly proposes that measurement disturbs the underlying hidden-variable distribution and achieves the full quantum correlation under a redefinition of locality that rejects counterfactual definiteness. We verified this model numerically and confirmed it reproduces both the correct transition curve and $S \approx 2.83$. We consider this a genuine precedent for the general strategy of modelling measurement as a disturbance to a hidden-variable distribution, but note a methodological distinction: the cited model's disturbance step directly incorporates the quantum mechanical transition probability, $\cos^2(\Delta\theta/2)$, as a postulated rule, whereas the derivation goal of the present work — consistent with the nuclear-mechanical account in Section 1 — is to obtain this probability as an emergent consequence of geometric and threshold-based construction rather than as an input.

6.6 Is This Model Local or Non-Local?

Whether this mechanism should be called “local” or “non-local” depends on which feature is treated as decisive, and the literature does not agree on this point. In favor of “local”: the dependency is fixed at a single, identifiable event at the particles' common origin, before separation (Section 6.2); nothing travels faster than light, and nothing needs to, since no signal crosses the distance between the separated particles at measurement time. In favor of “non-local”: the two particles' outcomes are not independent draws — one shared value determines both — and Bell's theorem establishes that no model in which each particle's outcome depends only on information generated independently for that particle can exceed the classical bound of 2 (Section 2). Because this model does exceed that bound (Section 5.2), it falls outside the class of models conventionally called “local” in the Bell sense, even though it avoids the superluminal signaling, backward-in-time influence, and cosmological pre-correlation associated with other non-local accounts (Section 6.5 above). We take no position on which usage is correct, and describe the mechanism's actual structure (Sections 6.1–6.2) so readers can apply whichever definition they find most useful.

7. Implications

We note briefly, and with appropriate caution, several established open questions in the foundations of quantum mechanics that a verified, physically-grounded mechanism of the kind proposed here would bear on, without claiming that the present work resolves any of them.

- The measurement problem. The trajectory-lock account of collapse described in Section 1.2, and verified computationally in Sections 4 and 5, provides a concrete, non-observer-dependent physical sequence — field competition, geometric consolidation, centrifugal stabilisation — in place of an unexplained collapse postulate. This bears directly on the measurement problem, though we note that a full account would additionally need to address the general quantum measurement formalism beyond the specific spin-measurement case treated here.
- The epistemic/ontic status of quantum probability. Because the present model proposes probability as arising from a genuine, underlying physical process (the partcile's orientation relative to a threshold) rather than as an irreducible feature of nature, it is naturally read as a contribution to the ontic side of this debate. We note this as a natural implication of the model's structure rather than as a claim independently argued for in this paper.
- Interpretation of the shared-value dependency. As discussed in Section 6.5, the present model identifies a minimal, specific dependency distinct from existing named categories, which may be of independent interest to the broader interpretation debate regardless of the model's ultimate physical correctness.
- Quantum gravity and unification. We explicitly do not claim the present work bears on the unification of quantum mechanics and general relativity. This is a substantially larger and physically distinct problem from spin correlation, and we flag its absence from the above list deliberately, to avoid overstating the scope of a model developed and verified specifically for the spin and entanglement case.

8. Limitations and Future Work

- The behavior of the mechanism under measurement settings changed after particle separation was tested for constructions in which the shared value cannot reference either setting (Section 6.2) — an internal consistency check only. Every such construction capped at the classical CHSH bound, consistent with Bell's theorem. This has no experimental point of comparison at present, and the photon-polarization case — a physically distinct system — remains untested and is not addressed by this result.
- The candidate trigger mechanisms identified in Section 6.3 remain numerically indistinguishable among those satisfying the spin-label-independence condition; identifying a testable point of divergence between them is a priority for future work.
- The photon/polarizer analogue of this mechanism, including the appropriate equivalent of a 'magnetic field' for a photon, has not been developed and is treated as a distinct undertaking.
- All results in this paper are Monte Carlo estimates (sample sizes of 60,000-300,000 trials per data point) rather than closed-form analytic derivations; an analytic treatment of the model, where tractable, would strengthen the precision of the reported curve-fit and CHSH values.
- The physical origin of the trigger event itself — why a variable fixed at the particles' common origin, rather than either particle's own subsequently-measured state, should determine which of two distant settings becomes generative — remains an open interpretive question, distinct from the structural/mathematical characterisation provided here.

9. Conclusion

We have presented a step-by-step mechanism, grounded in the nuclear-dynamical account of electron spin proposed in the Liquid Gravity Atomic framework, that reproduces the quantum mechanical prediction for sequential spin measurement without postulating the target formula directly, and an extension that reproduces the entangled-pair correlation to within 0.4% of the theoretical maximum, exceeding the classical bound of 2 available to any model in which each particle's outcome depends only on its own setting. Systematic testing locates the shared-value dependency required by the entangled case to a single, minimal point in the mechanism — the generation of one shared value from one magnet's setting, decided by a trigger fixed at the particles' common origin and independent of either particle's own spin label — distinguishing this model, which we term a Proximal Correlation Model, from superdeterminism, Bohmian mechanics, and retrocausal accounts. We regard the identification of this minimal step, the specific design constraints required to satisfy it (dynamic rather than fixed density generation; consistent behaviour under trigger substitution; independence of the trigger from either particle's spin label, confirmed by direct marginal-independence testing), and the transparent record of the iterative testing that located and corrected a violation of this last constraint, as the principal contributions of this work, and as a concrete, falsifiable target for future physical interpretation.

References

Aspect, A., Grangier, P., & Roger, G. (1982). Experimental Realization of Einstein-Podolsky-Rosen-Bohm Gedankenexperiment: A New Violation of Bell's Inequalities. Physical Review Letters, 49(2), 91-94.

Bell, J. S. (1964). On the Einstein Podolsky Rosen Paradox. Physics Physique Физика, 1(3), 195-200.

Bohm, D. (1952). A Suggested Interpretation of the Quantum Theory in Terms of 'Hidden' Variables, I and II. Physical Review, 85(2), 166-193.

Clauser, J. F., Horne, M. A., Shimony, A., & Holt, R. A. (1969). Proposed Experiment to Test Local Hidden-Variable Theories. Physical Review Letters, 23(15), 880-884.

Hensen, B., Bernien, H., Dréau, A. E., et al. (2015). Loophole-free Bell inequality violation using electron spins separated by 1.3 kilometres. Nature, 526(7575), 682-686.

Hodges, M. (2026). Resolving Spin and Entanglement with Testable Local Hidden Variables: The Liquid Gravity Atomic Model and a Proposed Stern-Gerlach Experiment Challenging Standard Probabilistic Predictions. ResearchGate.

Matzkin, A. (2007). A local model reproducing quantum correlations via measurement-induced disturbance of hidden variables. arXiv:quant-ph/0703271.